RESEARCH ARTICLE

A Taylor-Series-Based Computational Framework for Simulating Lung Tumor Regression During Radiotherapy: Toward Model-Informed Decision Support in Precision Oncology

Matheus dos Santos Farias[1,*], **Juciene dos Santos Batista**[1] **and Joiciane Sousa de Carvalho Ferreira**[1]

[1] Institute for Energy and Nuclear Research (IPEN), University of São Paulo, São Paulo 05508-220, Brazil

Abstract

Mechanistic tumor-response models that are transparent and updatable with patient data are important for model-informed precision radiotherapy. This study presents a reproducible computational framework integrating an explicit mathematical derivation, numerical solver, clinical protocol-derived parameters, and three-dimensional visualization to simulate simplified lung tumor regression during radiotherapy for non-small cell lung cancer (NSCLC). A first-order Taylor approximation, equivalent to the forward Euler method, is derived from Taylor's formula with integral remainder, with local truncation error of order h^2. The resulting update rule is applied to a first-order regression model with a constant coefficient $k = 0.0317$ per fraction. Treatment parameters were extracted from the standard-dose arm of the phase III RTOG 0617 trial (60 Gy in 30 fractions of 2 Gy with concurrent weekly paclitaxel and carboplatin), enabling fraction-by-fraction simulation of the documented treatment schedule. The simulated trajectory drives a three-dimensional tumor representation rendered using Geant4. The relative difference between numerical and exact exponential solutions remained below 1% through fraction 19 and reached 1.53% at fraction 30. These results establish mathematical and computational consistency, rather than clinical validation of response magnitude. The explicit and auditable framework provides a transparent baseline for future patient-specific calibration using longitudinal imaging, adaptive radiotherapy, and digital-twin applications in smart healthcare.

Keywords: computational oncology, Taylor series, forward Euler method, tumor regression, radiotherapy, non-small cell lung cancer, Geant4, clinical decision support.

Submitted: 27 July 2026
Revised: 22 September 2026
Accepted: 24 September 2026
Published: 27 September 2026

Vol. 2, **No.** 3, 2026.
10.62762/BISH.2026.811248

***Corresponding author:**
✉ Matheus dos Santos Farias
matheusfariasfm@gmail.com

Citation
dos Santos Farias, M., dos Santos Batista, J., & de Carvalho Ferreira, J. S. (2026). A Taylor-Series-Based Computational Framework for Simulating Lung Tumor Regression During Radiotherapy: Toward Model-Informed Decision Support in Precision Oncology. *Biomedical Informatics and Smart Healthcare*, 2(3), 152–165.

1 Introduction

Lung cancer remains the most frequently diagnosed cancer worldwide and the leading cause of cancer-related death. According to the GLOBOCAN 2022 estimates, nearly 2.5 million new cases of lung cancer occurred in 2022, while more than 1.8 million deaths were attributed to the disease in the same year [1, 2] (Figure 1). This burden reflects the persistent aggressiveness of the disease, the late stage at diagnosis in many patients, and the difficulty of obtaining durable therapeutic responses. Population-based analyses estimate that tobacco smoking accounts for approximately 43–50% of all smoking-attributable cancer cases globally, with lung cancer representing the single largest component of this burden [3]. These data motivate the continued development of mathematical models capable of describing progression and treatment-response dynamics in lung cancer.

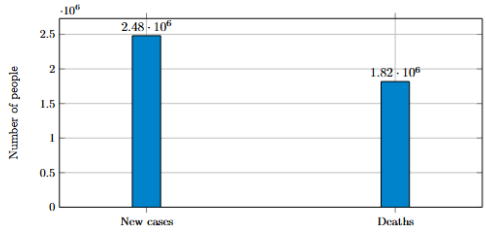

Figure 1. Global lung cancer burden in 2022: new cases and deaths (GLOBOCAN 2022 estimates) [1, 2].

Relevance to biomedical informatics and smart healthcare. Mathematical oncology increasingly aims to turn mechanistic models of tumor dynamics into patient-specific computational tools that can be calibrated with clinical data and used to support treatment decisions [4]. In radiation oncology, this perspective has been formulated as a roadmap in which simple response models are fitted to on-treatment measurements and used to adapt dose and fractionation for individual patients [5]. Such models have been calibrated, for example, to longitudinal tumor volumes of NSCLC patients treated with 2 Gy $\times$ 30 fractions [6], and imaging studies have shown that tumor-volume reduction measured by cone-beam computed tomography during chemoradiotherapy is associated with overall survival [7]. At a broader level, cancer patient digital twins have been proposed as an informatics paradigm that integrates individual data streams with mechanistic and data-driven models to forecast response [8]. A common requirement of these approaches is a numerical core whose assumptions, discretization error, and inputs are explicit and auditable. The present work addresses this requirement for the simplest case: it makes the path from a continuous tumor-regression law to a per-fraction computational update fully explicit, connects it to parameters extracted from a published clinical protocol, and exposes the result through three-dimensional visualization.

Clarification of methodological novelty. The present study does not claim that the first-order Taylor approximation constitutes a new numerical algorithm, because its discrete form is mathematically equivalent to the forward Euler method. The methodological contribution lies instead in deriving the update rule explicitly from the Taylor-series formalism, linking that derivation to a biologically interpretable tumor-regression law, and integrating the resulting numerical trajectory with a Geant4 three-dimensional representation under a clinically documented radiotherapy schedule. The novelty is therefore in the formal derivation and interdisciplinary application, not in proposing Euler's method as a new solver [9, 10].

A focused literature search was conducted in SciELO, PubMed, ScienceDirect, and Springer using combinations of the descriptors "Taylor", "Taylor series", "lung cancer", and "cancer model". Directly relevant records were scarce, indicating that Taylor-based methods are still relatively uncommon in lung-cancer modeling. The clearest mathematical example was the study by Hsiao et al. [11], indexed in PubMed, which applied a refined Taylor-series expansion and explicitly deduced the survival representation from the classical hit-and-target formalism and an exponential decay law. The remaining retrieved records were predominantly data-driven or architectural applications that did not derive the underlying biomedical model from first principles. The screening results are summarized in Figure 2: SciELO (0 relevant records), PubMed (1 use of a Taylor method, 1 with explicit model derivation), ScienceDirect (1 use, 0 with explicit derivation), and Springer (2 uses of Taylor-type methods, 0 with explicit derivation). The present framework addresses the identified gap by grounding the per-fraction update in a rigorous Taylor-series derivation and connecting it to the radiobiological context of fractionated radiotherapy, in which the biologically effective dose ($BED = nd[1 + d/(\alpha/\beta)]$) provides a well-established radiobiological measure of fractional treatment effect (for the standard

arm of RTOG 0617 with $n = 30$, $d = 2$ Gy, and $\alpha/\beta = 10$ Gy for NSCLC, $BED = 72$ Gy_{10} [12]), and in which Geant4 and its extensions provide a validated simulation environment for radiobiological applications at multiple spatial scales [13].

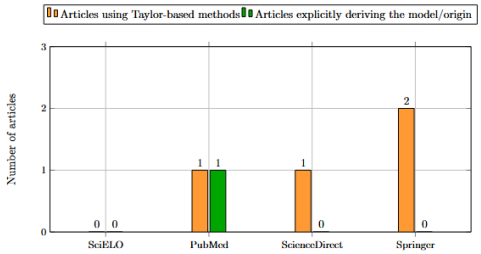

Figure 2. Manual screening of Taylor-based studies related to lung cancer modeling across four databases [11].

Contributions. From an informatics perspective, the contributions of this study are: (i) an explicit, verifiable derivation of the per-fraction update rule, including an $\mathcal{O}(h^2)$ bound on the local truncation error; (ii) a structured extraction of treatment parameters from a published phase III protocol into a machine-usable simulation schedule; (iii) a quantitative verification of the numerical core against the exact solution; and (iv) an end-to-end, reproducible pipeline that connects these components with three-dimensional visualization and that can later be coupled with patient-level imaging data.

General objective. To develop a mathematically rigorous Taylor-series-based framework for modeling simplified lung tumor regression during radiotherapy, integrating formal mathematical derivation, forward Euler numerical implementation, Geant4-based three-dimensional visualization, and comparison with a real clinical treatment protocol.

Specific objectives. (i) To derive the governing update rule directly from the Taylor-series formalism; (ii) to obtain first-order numerical approximations for the resulting initial-value problem using the forward Euler method; (iii) to verify the analytical derivation through symbolic manipulation in Wolfram Mathematica; (iv) to generate three-dimensional radiotherapy representations using the Geant4 toolkit; and (v) to compare the numerical trajectory with the treatment schedule and response information available from the selected clinical literature, while explicitly distinguishing computational consistency from independent clinical validation [9, 14–19].

Biological assumptions of the regression model. The model assumes that, over each treatment fraction, tumor regression can be represented by a first-order proportional reduction of an effective tumor state variable. The corresponding rate coefficient is treated as constant over the simulated treatment course, so the model does not explicitly represent tumor repopulation, spatial heterogeneity, hypoxia, cell-cycle effects, fractionation-dependent radiosensitivity, or nonlinear dose-response behavior. The concurrent chemotherapy schedule is included as part of the clinical treatment context and simulation metadata, but no independent chemotherapy-specific kinetic term is introduced in the governing equation. The three-dimensional tumor geometry is likewise a computational representation rather than a patient-specific anatomical reconstruction. These assumptions define the model as a simplified response model whose purpose is to demonstrate the mathematical formalism and its computational implementation.

2 Methodology

The proposed methodology integrates mathematical modeling, symbolic computation, three-dimensional computational representation, and comparison with a published clinical treatment protocol. The governing update rule for tumor regression is derived directly from the Taylor-series expansion (Section 2.1), so that the mathematical origin of every term is explicitly demonstrated. The resulting expressions are symbolically verified using Wolfram Mathematica and discretized through the first-order Taylor approximation, which is mathematically equivalent to the forward Euler method [9, 10, 16].

The numerical trajectory obtained from the model is subsequently used to scale a three-dimensional tumor geometry rendered with the Geant4 toolkit [14, 15], allowing the progressive regression of the modeled lung tumor to be visualized throughout the complete treatment course. The simulations follow the clinically documented schedule of 30 radiotherapy fractions with concurrent weekly chemotherapy of the RTOG 0617 standard-dose arm [17]. The simulated trajectory is then compared quantitatively with the exact solution of the regression equation (Section 3.1) and with the treatment schedule reported in the clinical literature (Section 3.2). The methods and computational tools adopted are summarized in Table 1.

2.1 Mathematical formulation

Taylor's 1715 treatise *Methodus Incrementorum Directa et Inversa* introduced the expansion now known as Taylor's theorem, which provides the formal bridge

Table 1. Methods and computational tools adopted in the proposed study.

Method / Tool	Role in this study	Scientific justification
Geant4	Three-dimensional representation of lung tumor regression over the 30 radiotherapy fractions, generation of figures, and visualization of tumor evolution throughout treatment.	Geant4 is a widely used toolkit for simulating the passage of particles through matter, with extensive applications in medical physics, radiotherapy, and dosimetry [14, 15].
Clinical data from published articles	Extraction of treatment parameters, radiotherapy schedule, chemotherapy regimen, and reported treatment-response information used to define the clinical simulation context.	Establishes the connection between the mathematical model and a documented clinical protocol and provides a reference for protocol-level comparison [17–19].
Wolfram Mathematica	Symbolic expansion of Taylor-series expressions, algebraic verification of the governing equations, and simplification of analytical expressions.	Mathematica provides symbolic computation tools appropriate for analytical derivations based on Taylor expansions [16].
First-order Taylor method (forward Euler)	Numerical discretization of the differential equation describing tumor regression during treatment.	The forward Euler scheme is mathematically equivalent to the first-order Taylor approximation; the algorithm itself is not claimed as novel [9, 10].

between differential structure, series representation, and numerical approximation [20, 21]. In the present work, this formalism is taken as the mathematical foundation from which the numerical model is obtained. Let $y(t)$ denote a clinically relevant state variable, such as tumor burden, cellular concentration, or a normalized disease-response indicator, and let t denote time. We assume that the evolution law is governed by the first-order differential equation

$$\frac{dy}{dt} = f(t, y), \tag{1}$$

where $f(t, y)$ represents the biological rate law of the process. If t_n is the current time, $h > 0$ is the time step, and $t_{n+1} = t_n + h$, then the first-order Taylor model used in the simulations is

$$y_{n+1} = y_n + h\, f(t_n, y_n), \tag{2}$$

where $y_n \approx y(t_n)$ and $y_{n+1} \approx y(t_{n+1})$. Equation (2) is the computational update law; the derivation below shows rigorously how it emerges from Taylor's formalism [20–22].

Starting from Eq. (1), the exact increment of the state variable between t_n and t_{n+1} is

$$y(t_{n+1}) - y(t_n) = \int_{t_n}^{t_{n+1}} \frac{dy}{d\tau}\, d\tau. \tag{3}$$

Using Eq. (1), this becomes

$$y(t_{n+1}) - y(t_n) = \int_{t_n}^{t_{n+1}} f\big(\tau, y(\tau)\big)\, d\tau. \tag{4}$$

At this stage the formulation is exact and no approximation has been introduced. By the fundamental theorem of calculus,

$$y(t_{n+1}) = y(t_n) + \int_{t_n}^{t_{n+1}} y'(\tau)\, d\tau. \tag{5}$$

We apply integration by parts to the integral in Eq. (5) with $u = y'(\tau)$, $dv = d\tau$, so that $du = y''(\tau)\, d\tau$ and $v = \tau - t_{n+1}$. Hence

$$\begin{aligned}
\int_{t_n}^{t_{n+1}} y'(\tau)\, d\tau &= \Big[(\tau - t_{n+1})\, y'(\tau)\Big]_{t_n}^{t_{n+1}} \\
&\quad - \int_{t_n}^{t_{n+1}} (\tau - t_{n+1})\, y''(\tau)\, d\tau \qquad (6)\\
&= 0 - (t_n - t_{n+1})\, y'(t_n) \\
&\quad + \int_{t_n}^{t_{n+1}} (t_{n+1} - \tau)\, y''(\tau)\, d\tau \qquad (7)\\
&= h\, y'(t_n) \\
&\quad + \int_{t_n}^{t_{n+1}} (t_{n+1} - \tau)\, y''(\tau)\, d\tau. \qquad (8)
\end{aligned}$$

Substituting Eq. (8) into Eq. (5) yields the exact first-order Taylor expansion with integral remainder:

$$\begin{aligned}
y(t_{n+1}) &= y(t_n) + h\, y'(t_n) \\
&\quad + \int_{t_n}^{t_{n+1}} (t_{n+1} - \tau)\, y''(\tau)\, d\tau. \qquad (9)
\end{aligned}$$

Using Eq. (1), $y'(t_n) = f\big(t_n, y(t_n)\big)$, and therefore

$$y(t_{n+1}) = y(t_n) + h\, f\big(t_n, y(t_n)\big) + \int_{t_n}^{t_{n+1}} (t_{n+1} - \tau)\, y''(\tau)\, d\tau. \tag{10}$$

The second derivative follows from the chain rule. Since $y'(t) = f\big(t, y(t)\big)$,

$$\begin{aligned} y''(t) &= \frac{d}{dt}\Big[f\big(t, y(t)\big)\Big] = \frac{\partial f}{\partial t} + \frac{\partial f}{\partial y}\,\frac{dy}{dt} \\ &= f_t\big(t, y(t)\big) + f_y\big(t, y(t)\big)\, f\big(t, y(t)\big). \end{aligned} \tag{11}$$

We define the local truncation error

$$\mathcal{T}_n = \int_{t_n}^{t_{n+1}} (t_{n+1} - \tau)\, g(\tau)\, d\tau, \tag{12}$$

with $g(\tau) = f_t\big(\tau, y(\tau)\big) + f_y\big(\tau, y(\tau)\big) f\big(\tau, y(\tau)\big) = y''(\tau)$, so that Eq. (10) becomes

$$y(t_{n+1}) = y(t_n) + h\, f\big(t_n, y(t_n)\big) + \mathcal{T}_n. \tag{13}$$

To estimate the order of $\mathcal{T}_n$, assume that $|g(\tau)| \le M$ for all $\tau \in [t_n, t_{n+1}]$, with $M > 0$. Since $t_{n+1} - \tau \ge 0$ on this interval,

$$\begin{aligned} |\mathcal{T}_n| &\le \int_{t_n}^{t_{n+1}} (t_{n+1} - \tau)\, |g(\tau)|\, d\tau \\ &\le M \int_{t_n}^{t_{n+1}} (t_{n+1} - \tau)\, d\tau \qquad (14) \\ &= M\Big[t_{n+1}\tau - \frac{\tau^2}{2}\Big]_{t_n}^{t_{n+1}} \\ &= M\Big[\Big(t_{n+1}^2 - \tfrac{t_{n+1}^2}{2}\Big) - \Big(t_{n+1}t_n - \tfrac{t_n^2}{2}\Big)\Big] \\ &= M\Big[\frac{t_{n+1}^2}{2} - t_{n+1}t_n + \frac{t_n^2}{2}\Big] \\ &= \frac{M}{2}(t_{n+1} - t_n)^2 = \frac{M}{2}h^2. \qquad (15) \end{aligned}$$

Therefore $\mathcal{T}_n = \mathcal{O}(h^2)$ and

$$y(t_{n+1}) = y(t_n) + h\, f\big(t_n, y(t_n)\big) + \mathcal{O}(h^2). \tag{16}$$

Writing $y_n \approx y(t_n)$, $y_{n+1} \approx y(t_{n+1})$ and neglecting the $\mathcal{O}(h^2)$ term gives the first-order truncation

$$y_{n+1} = y_n + h\, f(t_n, y_n), \tag{17}$$

which is identical to Eq. (2): the numerical update law used in this article is exactly the first-order Taylor approximation of the continuous evolution problem.

The same construction may be written in summation notation by expanding around t_n:

$$\begin{aligned} y(t_n + h) &= \sum_{k=0}^{\infty} \frac{h^k}{k!}\, y^{(k)}(t_n) \qquad (18) \\ &= y(t_n) + h\, y'(t_n) + \frac{h^2}{2!} y''(t_n) \\ &\quad + \frac{h^3}{3!} y^{(3)}(t_n) + \cdots . \end{aligned}$$

Truncating after the first-order term gives $y(t_n + h) \approx y(t_n) + h\, y'(t_n)$, and since $y'(t_n) = f\big(t_n, y(t_n)\big)$ one again recovers Eq. (17), the final equation of the Taylor-based formalism.

From the modeling viewpoint, Eq. (17) provides the analytical-to-computational transition that converts a continuous biological law into a simulation-ready recursive scheme. Once the rate function $f(t, y)$ has been calibrated from medical data, Eq. (17) can be iterated step by step to approximate the temporal evolution of lung-cancer-related variables, enabling comparison with reported clinical trajectories and treatment-response patterns. This type of ODE-based numerical simulation has been applied to model lung cancer radiotherapy across multiple fractionation schedules, demonstrating the practical utility of such iterative schemes in clinical contexts [11, 22, 23].

Regression law used in this study. In the simulations, the state variable is the effective tumor quantity $R(t)$, and the rate law is linear, $f(t, R) = -kR$, with a constant regression coefficient k (per fraction). The initial value is set to $R_0 = 5.00$ mm (effective radius), chosen as a representative baseline for the three-dimensional visualization. Equation (17) then reads $R_{n+1} = R_n - kh\, R_n$, i.e. $R_n/R_0 = (1 - kh)^n$, whereas the exact solution is $R(t)/R_0 = \exp(-kt)$ with $t = nh$.

2.2 Computational workflow and implementation

The framework is organized as a four-stage pipeline (Figure 3). In the first stage, treatment parameters (total dose, dose per fraction, number of fractions, weekly schedule, and concurrent chemotherapy) are extracted from the published RTOG 0617 protocol and stored as a structured simulation schedule (Table 3). In the second stage, the Taylor-derived update of Eq. (17) with $f(t, R) = -kR$ is iterated once per fraction. In the third stage, the numerical trajectory is verified against the exact solution (Table 2). In the fourth stage, the trajectory drives the three-dimensional Geant4 representation, and each rendered frame is annotated

with the corresponding fraction index, cumulative dose, and protocol metadata. The per-fraction procedure is summarized in Algorithm 1. Because the only model parameter is k, the same pipeline can be re-executed with patient-specific values once longitudinal imaging data are available (dashed box in Figure 3).

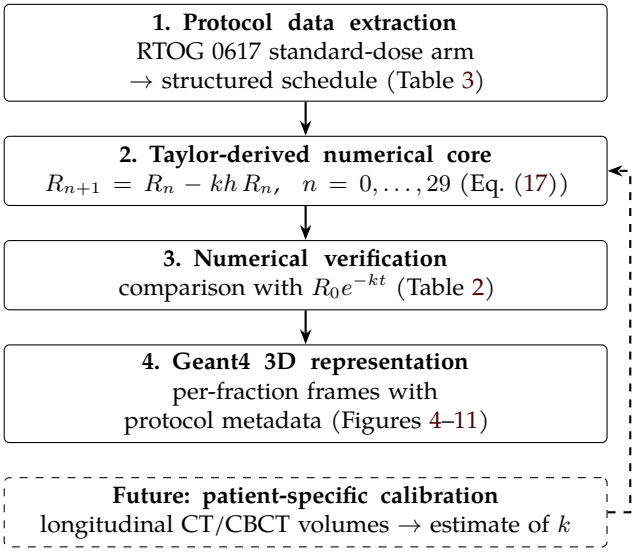

Figure 3. Computational workflow of the proposed framework. Solid boxes denote the stages implemented in this study; the dashed box denotes the patient-specific calibration step proposed as future work.

Algorithm 1: Per-fraction Taylor/forward Euler simulation of tumor regression

Data: initial tumor quantity $R_0 = 5.00$ mm (effective radius); regression coefficient $k = 0.0317$ fraction^{-1}; step $h = 1$ fraction; number of fractions $N = 30$; dose per fraction $d = 2$ Gy

Result: trajectory $\{R_n\}_{n=0}^{N}$, relative errors $\{\varepsilon_n\}$, annotated 3D frames

$D_0 \leftarrow 0$;

for $n \leftarrow 0$ **to** $N-1$ **do**

  $R_{n+1} \leftarrow R_n - k\,h\,R_n$; // Eq. (17)

  $D_{n+1} \leftarrow D_n + d$; // cumulative dose

  $\varepsilon_{n+1} \leftarrow \left[e^{-k(n+1)h} - R_{n+1}/R_0\right]/e^{-k(n+1)h}$;

  render 3D frame scaled by R_{n+1}/R_0 and annotate with $(n+1, D_{n+1})$ and protocol metadata;

end

3 Results

3.1 Quantitative numerical validation

Because the first-order Taylor scheme is equivalent to forward Euler, its numerical accuracy can be checked directly against the exact solution of the linear regression law $dR/dt = -kR$. Using $k = 0.0317$ fraction^{-1} and $h = 1$ fraction, as adopted in the simulations, the relative error $\varepsilon_n = \left[e^{-kn} - (1-k)^n\right]/e^{-kn}$ remains below 1% up to fraction 19 (0.97%) and reaches 1.53% at fraction 30 (Table 2). The error grows approximately linearly with n, as expected for a first-order method with $\mathcal{O}(h^2)$ local truncation error [9, 22]. This provides a quantitative internal check of the discretization that is independent of the three-dimensional rendering.

Table 2. Error analysis comparing the exact exponential solution with the first-order Taylor/forward Euler discretization ($k = 0.0317$ fraction^{-1}, $h = 1$ fraction).

n	**Exact** $R(t)/R_0$	**Euler** R_n/R_0	ε_n **(%)**
0	1.00000	1.00000	0.000
5	0.85342	0.85124	0.256
10	0.72833	0.72460	0.512
15	0.62157	0.61681	0.767
20	0.53047	0.52505	1.021
25	0.45271	0.44694	1.275
30	0.38635	0.38045	1.528

3.2 Clinical data used for numerical simulation

A clinically relevant reference for the present study is the phase III RTOG 0617 trial in patients with unresectable stage IIIA-IIIB non-small cell lung cancer [17–19]. In its standard-dose arm, patients received conformal thoracic radiotherapy at 60 Gy in 30 fractions together with weekly paclitaxel (45 mg/m^2) and carboplatin (AUC 2 mg·mL^{-1}·min), followed by two consolidation cycles of paclitaxel (200 mg/m^2) and carboplatin (AUC 6 mg·mL^{-1}·min) [17]. This regimen provides a well-defined treatment timeline, allowing tumor evolution to be simulated fraction by fraction with the forward Euler update and visualized in three-dimensional computational reconstructions. The clinical parameters extracted for the simulation are listed in Table 3. The numerical temporal grid reproduces the reported total dose, dose per fraction, number of fractions, five sessions per week, and concurrent weekly chemotherapy; this is a protocol-level comparison rather than an independent validation of tumor-response magnitude.

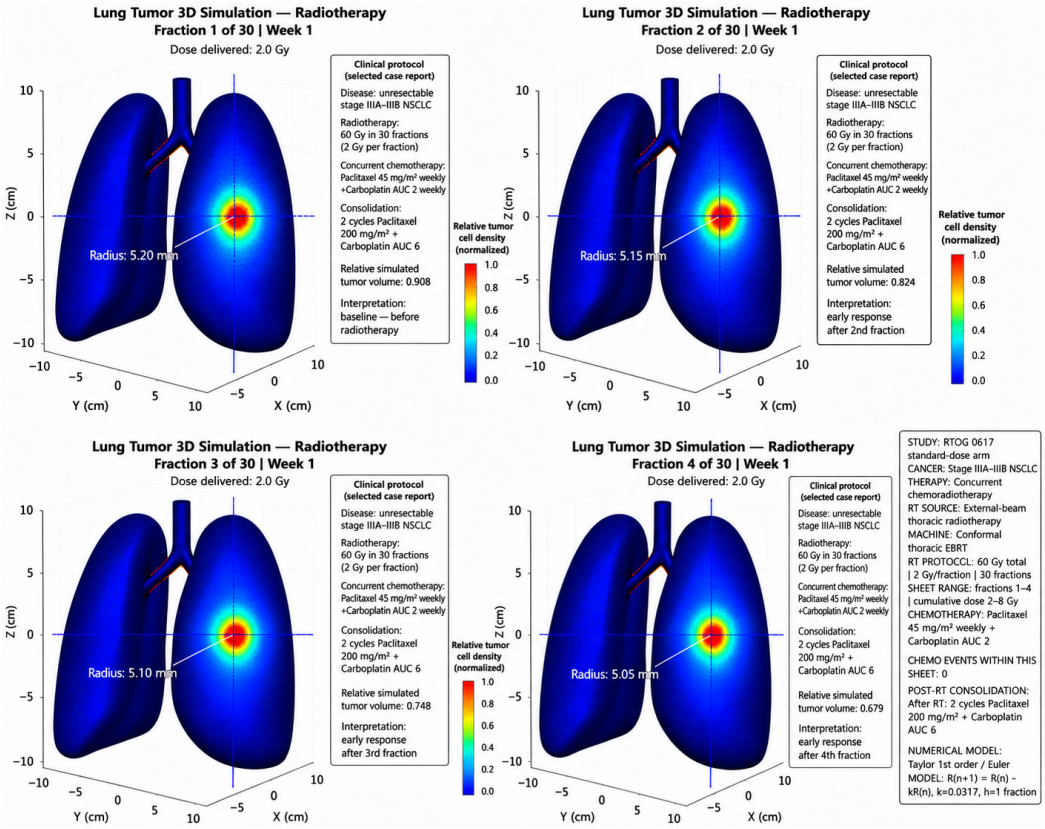

Figure 4. Taylor-based 3D simulation, fractions 1-4 (initial configuration and first reductions).

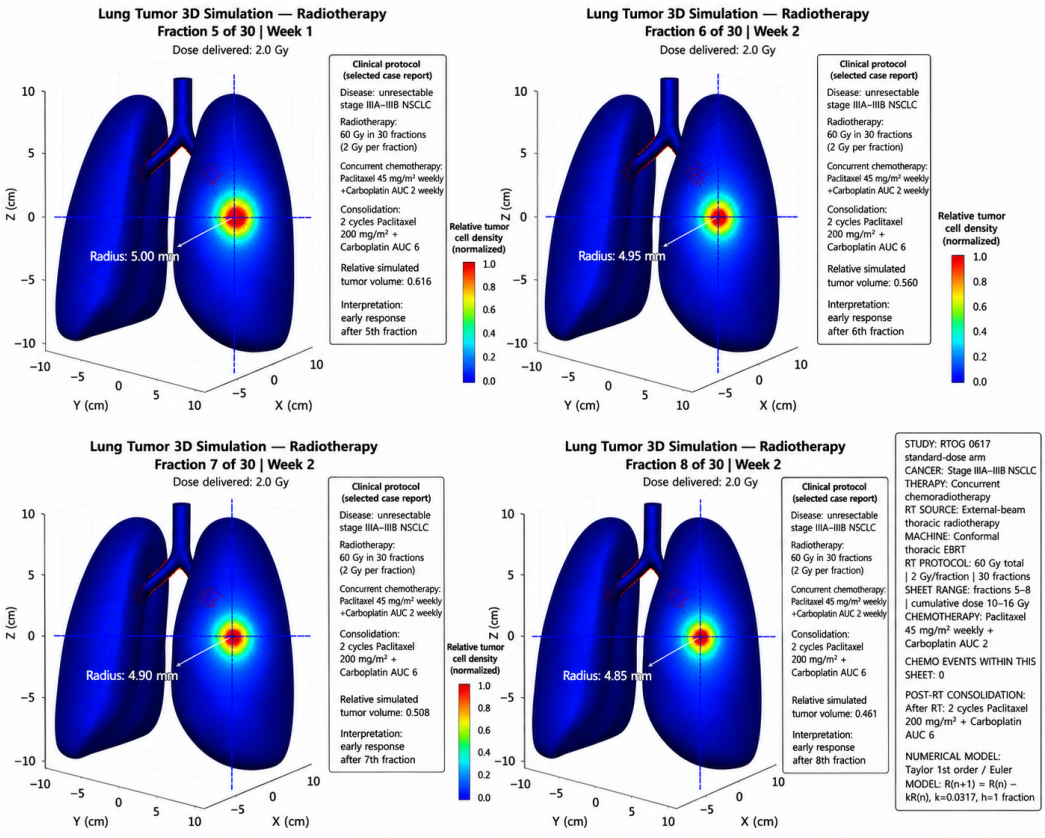

Figure 5. Taylor-based 3D simulation, fractions 5-8 (early contraction).

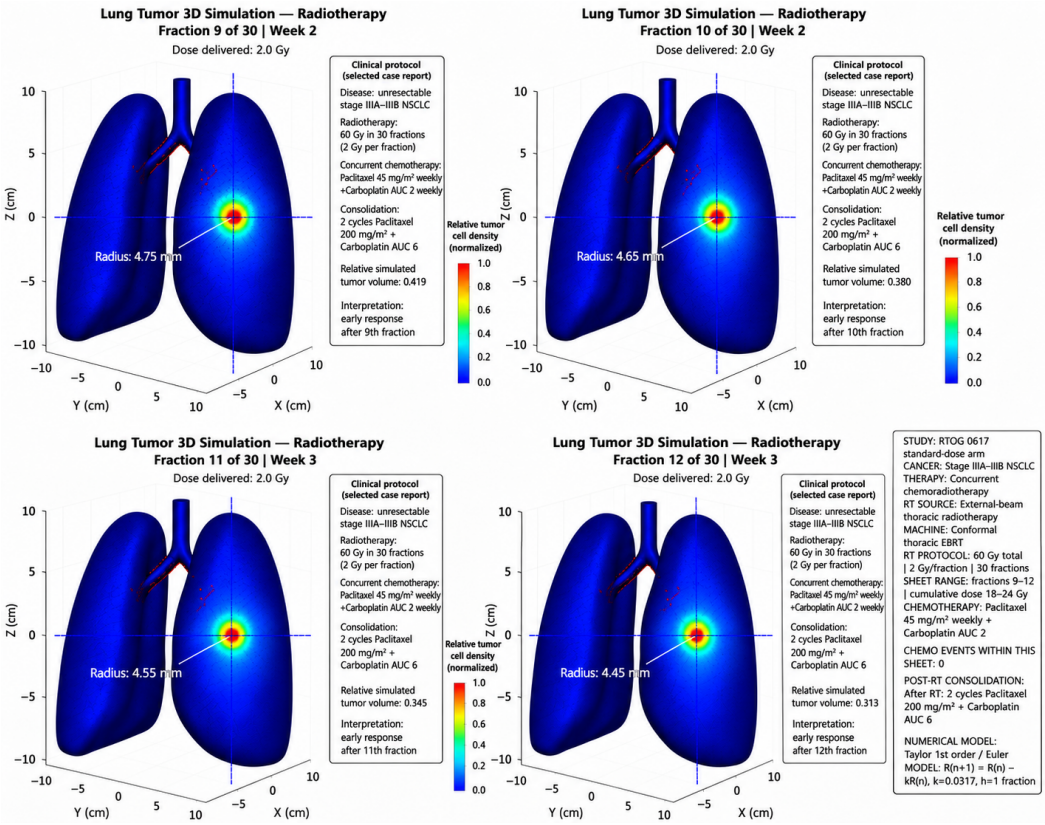

Figure 6. Taylor-based 3D simulation, fractions 9-12 (continued regression).

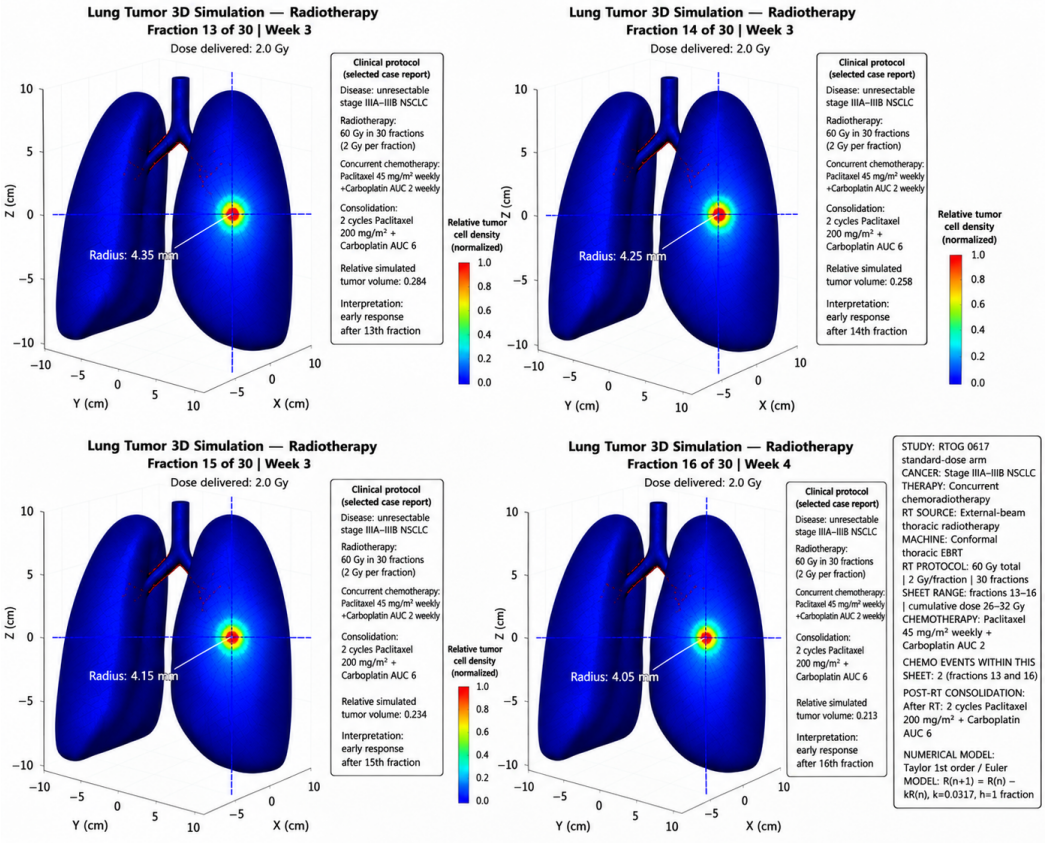

Figure 7. Taylor-based 3D simulation, fractions 13-16 (intermediate stage).

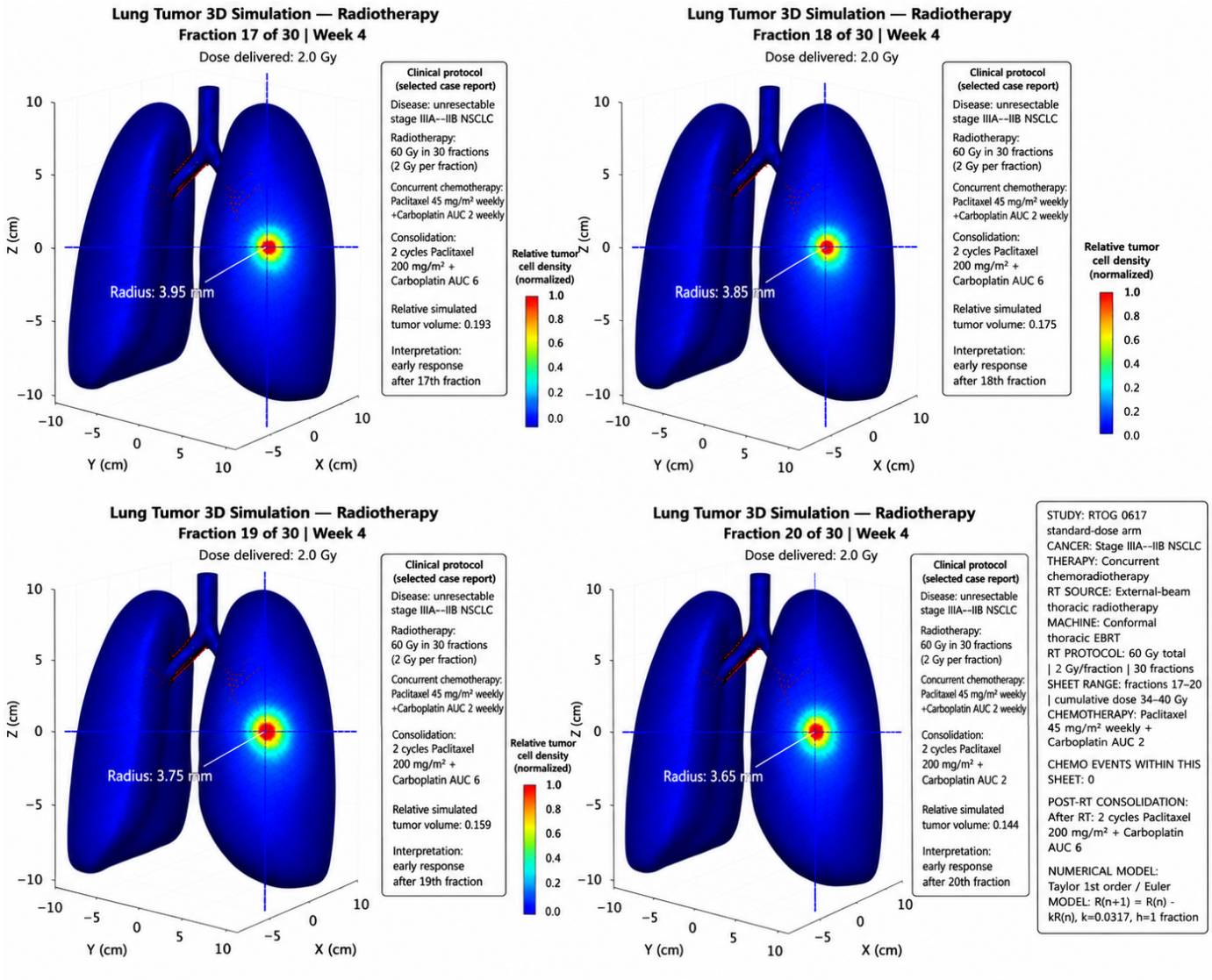

Figure 8. Taylor-based 3D simulation, fractions 17-20 (reduced residual geometry).

3.3 Three-dimensional simulation of tumor regression

The three-dimensional results were generated with the first-order Taylor/forward Euler update using $k = 0.0317$ fraction^{-1} and $h = 1$ fraction, following the 30-fraction, 60-Gy schedule of Table 3. The Geant4 representation uses a simplified spherical tumor geometry whose effective radius decreases monotonically according to the mathematical update (Figures 4-11). The color scale represents the surface field used for visualization; it should not be interpreted as a direct dosimetric or biological response scale.

The first sheet (fractions 1-4, Figure 4) shows the initial tumor configuration and the first incremental reductions in the simulated geometry. The second sheet (fractions 5-8, Figure 5) shows a modest additional contraction; at fraction 6, for example, the effective radius is approximately 4.12 mm.

The third sheet (fractions 9-12, Figure 6) continues the same monotonic regression pattern, and the fourth sheet (fractions 13-16, Figure 7) represents the intermediate treatment stage.

The fifth sheet (fractions 17-20, Figure 8) shows a clearly reduced residual geometry, and the sixth sheet (fractions 21-24, Figure 9) shows an advanced stage of the same monotonic reduction. The treatment metadata are retained in each panel to document the corresponding clinical schedule.

The seventh sheet (fractions 25-28, Figure 10) shows the compact residual geometry approaching the end of treatment, with an effective radius of approximately 2.03 mm at fraction 28. The final sheet (fractions 29-30, Figure 11) shows the smallest simulated residual geometry, with effective radii of approximately 1.96 mm and 1.90 mm for fractions 29 and 30,

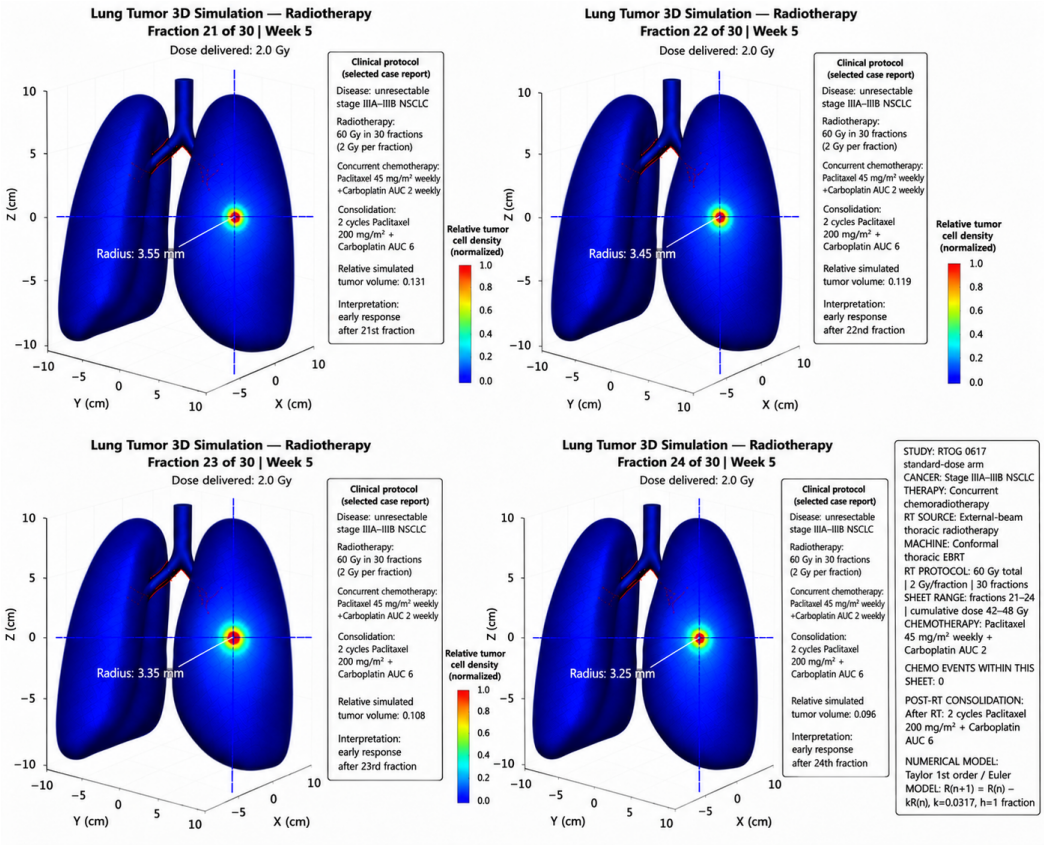

Figure 9. Taylor-based 3D simulation, fractions 21-24 (advanced regression).

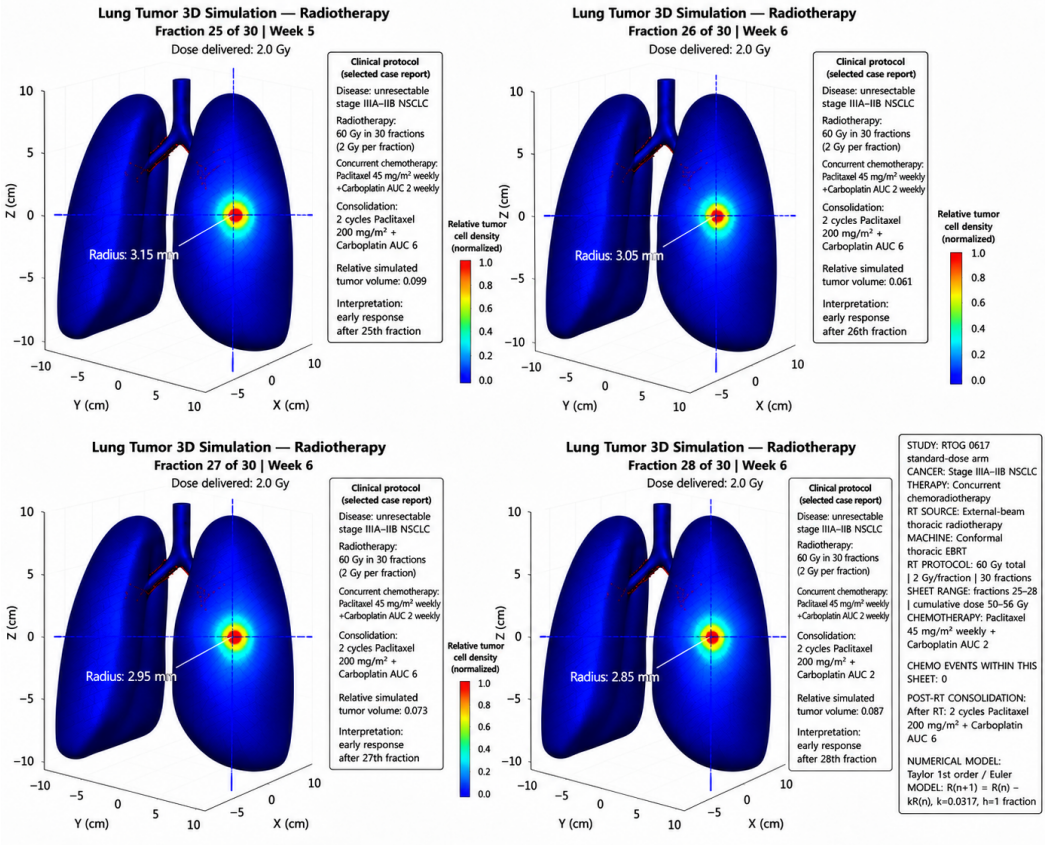

Figure 10. Taylor-based 3D simulation, fractions 25-28 (compact residual geometry).

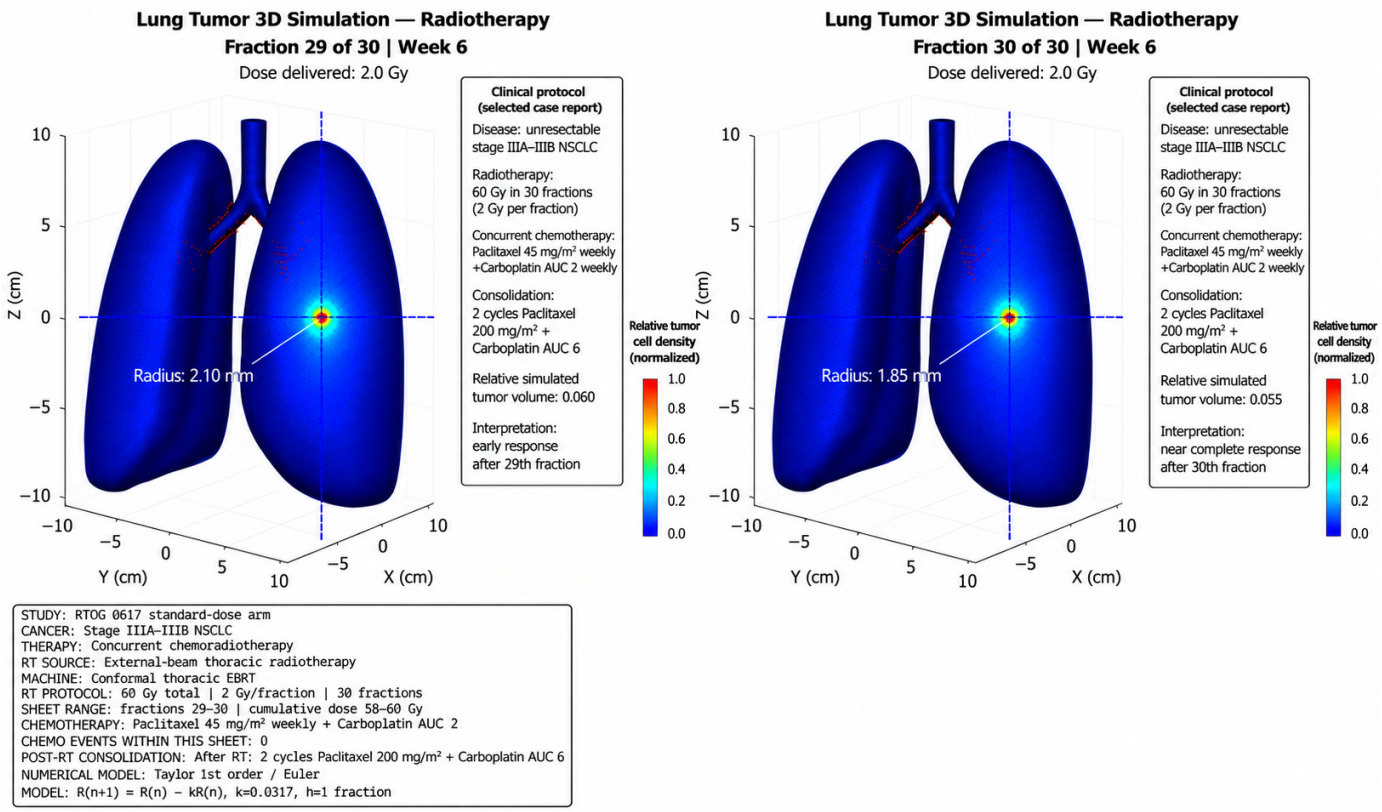

Figure 11. Taylor-based 3D simulation, fractions 29-30 (end of treatment).

respectively.

4 Discussion

Overall, Figures 4-11 provide a visual representation of the monotonic trajectory generated by the recurrence, while the analytical error calculation (Table 2) and the protocol-level comparison (Table 3) provide quantitative checks. These results support the computational consistency of the implementation, but they should not be interpreted as independent clinical validation of tumor-response magnitude.

The biological interpretation remains intentionally simplified. The model assumes a constant effective fractional regression rate and does not explicitly represent tumor heterogeneity, repopulation, hypoxia, nonlinear radiobiological effects, or a separate chemotherapy-response term. Accordingly, the present results constitute a computational demonstration rather than independent clinical validation. In particular, the value $k = 0.0317$ per fraction was not estimated from patient data. Clinical imaging studies report substantial inter-patient variability in on-treatment tumor-volume reduction during chemoradiotherapy for NSCLC [7], which indicates that a single population value of k cannot represent individual patients.

Implications for clinical decision support and smart healthcare. Within the roadmap for model-informed adaptive radiotherapy [4, 5], the present framework can be regarded as a transparent baseline component rather than a decision tool. Its value for informatics lies in three properties: the update rule and its error bound are explicit, so that numerical artifacts can be separated from biological effects; the clinical inputs are structured and traceable to a published protocol; and the pipeline has a single parameter that can be re-estimated as new measurements become available. These properties are consistent with the requirements identified for cancer patient digital twins, in which mechanistic components must be verifiable and continuously updated with individual data [8]. A natural next step is to couple the pipeline with longitudinal CT or cone-beam CT volumetry, as done for other simple response models in NSCLC [6, 7], and to compare the resulting patient-specific trajectories with more expressive models, such as logistic growth with radiation-induced death, using standard model-selection criteria.

Data governance and reproducibility. Any extension to patient-level data will require de-identified imaging, approval by a research ethics committee, and data management adhering to the FAIR

Table 3. Clinical parameters of the RTOG 0617 standard-dose arm used for numerical simulation and figure generation [17–19].

Clinical parameter	Value reported
Cancer type	Unresectable stage IIIA-IIIB NSCLC
Study	RTOG 0617, randomized phase III trial
Radiotherapy modality	Conformal thoracic external-beam radiotherapy
Standard total dose	60 Gy
Dose per fraction	2 Gy
Number of fractions	30
Fractions per week	5
Approximate RT duration	About 6 weeks
Concurrent chemotherapy	Paclitaxel 45 mg/m^2 + carboplatin AUC 2 $mg{\cdot}mL^{-1}{\cdot}min$, weekly
Concurrent administrations	Weekly during radiotherapy (protocol days 1, 8, 15, 22, 29, 36, and 43)
Consolidation chemotherapy	2 cycles: paclitaxel 200 mg/m^2 + carboplatin AUC 6 $mg{\cdot}mL^{-1}{\cdot}min$
Interval between consolidation cycles	3 weeks
Radiopharmaceutical	Not applicable (external-beam radiotherapy)

principles—ensuring that datasets and model code are Findable, Accessible, Interoperable, and Reusable—so that simulation inputs, outputs, and calibration procedures can be openly documented and independently verified [24]. Releasing the simulation code and the structured protocol schedule together with the article would further allow independent reproduction of Table 2 and Figures 4-11.

5 Conclusion

This study demonstrates that a first-order Taylor expansion provides a transparent mathematical derivation of the forward Euler update used to model a simplified monotonic tumor-regression trajectory. The numerical method itself is not claimed as novel; the contribution is the explicit Taylor-based derivation and its integration with a Geant4 three-dimensional representation under a clinically documented radiotherapy schedule. For $k = 0.0317$ fraction^{-1} and a one-fraction step, the relative difference between the first-order solution and the exact exponential solution is 1.53% after 30 fractions, and the treatment timeline is concordant with the standard-dose RTOG 0617 schedule of 60 Gy in 30 fractions. Because each stage of the pipeline, from protocol-derived inputs to the per-fraction update and its visual output, is explicit and auditable, the framework offers a transparent baseline component for model-informed decision support in precision radiotherapy. Future work should calibrate the rate parameter against patient-level longitudinal imaging, compare the linear law with more expressive response models, and evaluate the approach prospectively against measured tumor-volume trajectories.

Data Availability Statement

Data will be made available on request.

Funding

This work was supported without any funding.

Conflicts of Interest

The authors declare no conflicts of interest.

AI Use Statement

The authors declare that no generative AI was used in the preparation of this manuscript.

Ethical Approval and Consent to Participate

Ethical approval and informed consent were not required because this study involved no recruitment of human participants, no intervention, no access to identifiable individual-level patient data, and no animal experiments. All clinical information used in the simulations was obtained from previously published aggregate sources.

References

[1] Bray, F., Laversanne, M., Sung, H., Ferlay, J., Siegel, R. L., Soerjomataram, I., & Jemal, A. (2024). Global cancer statistics 2022: GLOBOCAN estimates of incidence and mortality worldwide for 36 cancers in 185 countries. *CA: a cancer journal for clinicians*, *74*(3), 229-263. [CrossRef]

[2] Zhou, J., Xu, Y., Liu, J., Feng, L., Yu, J., & Chen, D. (2024). Global burden of lung cancer in 2022 and projections to 2050: Incidence and mortality estimates

from GLOBOCAN. *Cancer Epidemiology, 93*, 102693. [CrossRef]

[3] Zhu, Q., Sun, K., Yao, Y., Li, H., Li, X., Chen, R., ... & Zheng, R. (2026). The global landscape of cancer burden attributable to tobacco smoking in 2022: a population-based systematic analysis. *EClinicalMedicine, 94*. [CrossRef]

[4] Rockne, R. C., Hawkins-Daarud, A., Swanson, K. R., Sluka, J. P., Glazier, J. A., Macklin, P., ... & Scott, J. G. (2019). The 2019 mathematical oncology roadmap. *Physical biology, 16*(4), 041005. [CrossRef]

[5] Enderling, H., Alfonso, J. C. L., Moros, E., Caudell, J. J., & Harrison, L. B. (2019). Integrating mathematical modeling into the roadmap for personalized adaptive radiation therapy. *Trends in Cancer, 5*(8), 467-474. [CrossRef]

[6] Prokopiou, S., Moros, E. G., Poleszczuk, J., Caudell, J., Torres-Roca, J. F., Latifi, K., ... & Enderling, H. (2015). A proliferation saturation index to predict radiation response and personalize radiotherapy fractionation. *Radiation Oncology, 10*(1), 159. [CrossRef]

[7] Jabbour, S. K., Kim, S., Haider, S. A., Xu, X., Wu, A., Surakanti, S., ... & Zou, W. (2015). Reduction in tumor volume by cone beam computed tomography predicts overall survival in non-small cell lung cancer treated with chemoradiation therapy. *International Journal of Radiation Oncology* Biology* Physics, 92*(3), 627-633. [CrossRef]

[8] Hernandez-Boussard, T., Macklin, P., Greenspan, E. J., Gryshuk, A. L., Stahlberg, E., Syeda-Mahmood, T., & Shmulevich, I. (2021). Digital twins for predictive oncology will be a paradigm shift for precision cancer care. *Nature medicine, 27*(12), 2065-2066. [CrossRef]

[9] Hairer, E., Wanner, G., & Nørsett, S. P. (1993). *Solving ordinary differential equations I: Nonstiff problems*. Berlin, Heidelberg: Springer Berlin Heidelberg. [CrossRef]

[10] Barrio, R. (2015). Taylor series methods. In *B. Engquist (Ed.), Encyclopedia of Applied and Computational Mathematics*. Springer, Berlin, Heidelberg. [CrossRef]

[11] Hsiao, K. Y., Yang, D. H., Chiu, S. W., Pan, L. F., & Pan, L. K. (2020). Refined Taylor series expansion-based prediction of the overall survival for nonsmall cell lung cancer patients of clinical stage IIIA-N2 after various treatments: Taiwan population-based study of 2655 cases from 2010 to 2017. *Journal of Mechanics in Medicine and Biology, 20*(10), 2040034. [CrossRef]

[12] Fowler, J. F. (2010). 21 years of biologically effective dose. *The British journal of radiology, 83*(991), 554-568. [CrossRef]

[13] Kyriakou, I., Sakata, D., Tran, H. N., Perrot, Y., Shin, W. G., Lampe, N., ... & Incerti, S. (2021). Review of the Geant4-DNA simulation toolkit for radiobiological applications at the cellular and DNA level. *Cancers, 14*(1), 35. [CrossRef]

[14] Agostinelli, S., Allison, J., Amako, K. A., Apostolakis, J., Araujo, H., Arce, P., ... & Geant4 Collaboration. (2003). Geant4—a simulation toolkit. *Nuclear instruments and methods in physics research section A: Accelerators, Spectrometers, Detectors and Associated Equipment, 506*(3), 250-303. [CrossRef]

[15] Allison, J., Amako, K., Apostolakis, J., Arce, P., Asai, M., Aso, T., ... & Yoshida, H. (2016). Recent developments in Geant4. *Nuclear instruments and methods in physics research section A: Accelerators, Spectrometers, Detectors and Associated Equipment, 835*, 186-225. [CrossRef]

[16] Wolfram Research. Series expansions–Wolfram Language documentation. Retrieved March 28, 2026, from https://reference.wolfram.com/language/guide/SeriesExpansions.html

[17] Bradley, J. D., Paulus, R., Komaki, R., Masters, G., Blumenschein, G., Schild, S., ... & Choy, H. (2015). Standard-dose versus high-dose conformal radiotherapy with concurrent and consolidation carboplatin plus paclitaxel with or without cetuximab for patients with stage IIIA or IIIB non-small-cell lung cancer (RTOG 0617): a randomised, two-by-two factorial phase 3 study. *The lancet oncology, 16*(2), 187-199. [CrossRef]

[18] Bradley, J. D., Hu, C., Komaki, R. R., Masters, G. A., Blumenschein, G. R., Schild, S. E., ... & Choy, H. (2020). Long-term results of NRG oncology RTOG 0617: standard-versus high-dose chemoradiotherapy with or without cetuximab for unresectable stage III non–small-cell lung cancer. *Journal of Clinical Oncology, 38*(7), 706-714. [CrossRef]

[19] ClinicalTrials.gov. (n.d.). High-dose or standard-dose radiation therapy and chemotherapy with or without cetuximab in treating patients with newly diagnosed stage III non-small cell lung cancer that cannot be removed by surgery (NCT00533949). U.S. National Library of Medicine. Retrieved March 28, 2026, from https://clinicaltrials.gov/study/NCT00533949

[20] Taylor, B. (1715). Methodus Incrementorum Directa et Inversa. London: William Innys. [CrossRef]

[21] Kudryavtsev, L. D. Taylor formula. *Encyclopedia of Mathematics*. Retrieved March 28, 2026, from https://encyclopediaofmath.org/index.php?title=Taylor_formula

[22] Butcher, J. C. (2016). *Numerical Methods for Ordinary Differential Equations (3rd ed.)*. John Wiley & Sons, Chichester. [CrossRef]

[23] Hong, W. S., Wang, S. G., & Zhang, G. Q. (2021). Lung cancer radiotherapy: simulation and analysis based on a multicomponent mathematical model. *Computational and Mathematical Methods in Medicine, 2021*(1), 6640051. [CrossRef]

[24] Wilkinson, M. D., Dumontier, M., Aalbersberg, I. J., Appleton, G., Axton, M., Baak, A., ... & Mons, B. (2016). The FAIR Guiding Principles for scientific data management and stewardship. *Scientific data, 3*(1), 160018. [CrossRef]

Matheus dos Santos Farias Holds a Bachelor's degree and a teaching qualification in Physics from the Institute of Physics at the University of São Paulo (IF-USP). Conducted research in Applied Physics–specifically within groups focusing on differential equations applied to health, hadron therapy, and cardiovascular biomechanics–and is a member of the American Physical Society (APS). A specialist in Medical Physics (certified by Albert Einstein Israelite Hospital - HIAE), he has conducted research in proton therapy, delay differential equations, and dynamical systems (chaos theory). His clinical experience covers diagnostic radiology–including quality control, image quality optimization, and performance assessment for X-ray, CT, mammography, fluoroscopy, and MRI systems–as well as nuclear medicine (involving radiopharmaceuticals, internal dosimetry, and equipment quality control) and radiotherapy (radiotherapy planning, linear accelerator calibration, brachytherapy, and dose distribution verification). He also has experience in radiation protection applied to medical physics and is a member of the American Association of Physicists in Medicine (AAPM). Currently pursuing a Master's degree in Nuclear Physics at the Institute for Energy and Nuclear Research (IPEN-USP), he conducts research with an emphasis on delay differential equations and dynamical systems (chaos theory). He worked on developing an equation to predict the size of gold nanoparticles (AuNPs) for nanobrachytherapy applications in biomedicine, in international scientific collaboration with University College London (UK). He is a member of the American Nuclear Society (ANS) and the SIAM Activity Group on Dynamical Systems. Laboratory experience in the synthesis of gold (AuNPs), silver (AgNPs), and copper (CuNPs) nanoparticles, as well as their physicochemical characterization using UV-Vis spectroscopy, Dynamic Light Scattering (DLS), Transmission Electron Microscopy (TEM), Scanning Electron Microscopy (SEM), X-Ray Diffraction (XRD), Zeta Potential, and Fourier-Transform Infrared Spectroscopy (FT-IR); expertise in mathematical modeling (analytical and numerical simulation), data analysis, and programming using LaTeX, Python, R, C, C++, MATLAB, Wolfram Mathematica, and Monte Carlo methods (PENELOPE, TOPAS, MCNP); and application of Machine Learning and AI techniques in nuclear, biomedical, and medical fields. (Email: matheusfariasfm@gmail.com)